RADC-TR-78-42
IN HOUSE REPORT
FEBRUARY 1978

LEVEL II

11

12 44p.

A Diffraction Analysis of the Elliptical Reflector.

9 Technical rept.,

RONALD L. FANTE

ROME AIR DEVELOPMENT CENTER
AIR FORCE SYSTEMS COMMAND
GRIFFISS AIR FORCE BASE, NEW YORK 13441

Title of Report: A Diffraction Analysis of the Elliptical Reflector

This Technical Report has been reviewed and approved for publication.

APPROVED:

Walter Rotman

WALTER ROTMAN, Chief
Antennas and RF Components Branch
Electromagnetic Sciences Division

APPROVED:

Allan C. Schell

ALLAN C. SCHELL, Acting Chief
Electromagnetic Sciences Division

FOR THE COMMANDER: John P. Huss

Plans Office

Unclassified

SECURITY CLASSIFICATION OF THIS PAGE (When Data Entered)

REPORT DOCUMENTATION PAGE		READ INSTRUCTIONS BEFORE COMPLETING FORM
1. REPORT NUMBER RADC-TR-78-42	2. GOVT ACCESSION NO.	3. RECIPIENT'S CATALOG NUMBER
4. TITLE (and Subtitle) A DIFFRACTION ANALYSIS OF THE ELLIPTICAL REFLECTOR		5. TYPE OF REPORT & PERIOD COVERED In-House Report 6. PERFORMING ORG. REPORT NUMBER
7. AUTHOR(s) Ronald L. Fante		8. CONTRACT OR GRANT NUMBER(s)
9. PERFORMING ORGANIZATION NAME AND ADDRESS Deputy for Electronic Technology (RADC/EEA) Hanscom AFB Massachusetts 01731		10. PROGRAM ELEMENT, PROJECT, TASK AREA & WORK UNIT NUMBERS 61102F 2305J303
11. CONTROLLING OFFICE NAME AND ADDRESS Deputy for Electronic Technology (RADC/EEA) Hanscom AFB Massachusetts 01731		12. REPORT DATE February 1978 13. NUMBER OF PAGES 39
14. MONITORING AGENCY NAME & ADDRESS(if different from Controlling Office)		15. SECURITY CLASS. (of this report) Unclassified 15a. DECLASSIFICATION/DOWNGRADING SCHEDULE
16. DISTRIBUTION STATEMENT (of this Report) Approved for public release; distribution unlimited.		
17. DISTRIBUTION STATEMENT (of the abstract entered in Block 20, if different from Report)		
18. SUPPLEMENTARY NOTES		
19. KEY WORDS (Continue on reverse side if necessary and identify by block number) Antennas Reflectors Diffraction		

20. ABSTRACT (Continue on reverse side if necessary and identify by block number)

A study has been made of the distribution of the electromagnetic fields diffracted by an elliptical reflector that is fed by a source at or near one of its two foci. For both the elliptic cylinder and the ellipsoid of revolution, the following calculations have been made: the magnitude of the fields near the foci, the size of the focal region, the displacement of the focal spot as a function of the source displacement, and application of the method of stationary phase in calculating the fields at points distant from either focus. Explicit results are → next page

DD FORM 1 JAN 73 1473 EDITION OF 1 NOV 65 IS OBSOLETE

Unclassified

SECURITY CLASSIFICATION OF THIS PAGE (When Data Entered)

20. Abstract (Continued)

presented for the fields as a function of the eccentricity of the ellipse and the angles subtended by the reflector edges.

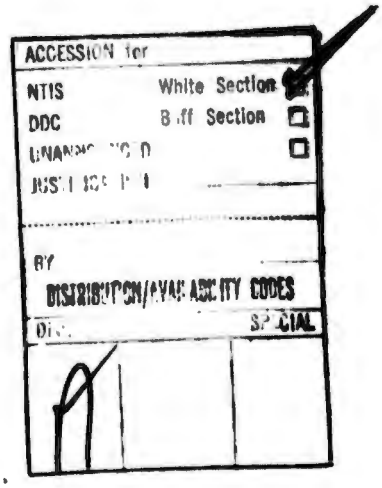

Contents

Illustrations

A Diffraction Analysis of the Elliptical Reflector

1. INTRODUCTION

Recently, a number of applications have arisen for which a reflector system with two foci, such as an ellipse, seems attractive. Among these are runway surveillance, perimeter systems for base security, and illumination of biological specimens. In this system, the feed is placed at or near one focus and the second focus is placed at the region we desire to illuminate. Unfortunately, the field distribution of the elliptical reflector does not appear to have been studied in any detail, and the literature on this subject is scant;[1] the bulk of the analysis has been devoted[2-5] to the more familiar parabolic reflector, which has its second focus at infinity. Therefore, in this paper we will perform a detailed study of the field distribution of both the elliptic cylinder and the ellipsoid of revolution.

(Received for publication 28 February 1978)

1. Soejima, T. (1973) Scattering by two elliptical reflectors; correspondence with diffraction by two circular apertures, IEEE Trans Ant. Prop. 21:110-113.

2. Sletten, C.J. (1969) Reflector antennas, in Antenna Theory, Part 2, R. Collin and F. Zucker, Ed., McGraw-Hill, New York.

3. Minnett, H., and Thomas, B. Mac A. (1968) Fields in the image plane of symmetrical focusing reflectors, Proc. IEE 115:1419-1430.

4. Rusch, W., and Potter, P. (1970) Analysis of Reflector Antennas, Academic Press, New York.

5. Clarricoats, P., and Poulton, G. (1977) High-efficiency microwave reflector antennas - a review, Proc. IEEE 65:1470-1504.

2. THE ELLIPTIC CYLINDER

2.1 Analytical Preliminaries

The magnetic field scattered by a cylindrical reflector having a surface satisfying the equation $z = f(x)$ can be written* as[6]

$$\underline{H}(x', z') = -\left(\frac{ik}{2\pi}\right)^{1/2} \int dx \left\{\left(\hat{z} - \hat{x}\,\frac{\partial f}{\partial x}\right) \times \underline{H}_i\right\} \times \left\{\frac{(x' - x)\hat{x} + (z' - z)\hat{z}}{\rho}\right\} \frac{e^{-ik\rho}}{(\rho)^{1/2}} \quad , \tag{1}$$

where $\underline{H}_i$ is the magnetic field of the wave incident upon the reflector, ρ is the distance from the point (x, z) on the reflector to the field point (x', z'), k the signal wave number and $\hat{x}, \hat{z}$ are unit vectors in the x and z directions, respectively. We will now apply Eq. (1) to obtain the field scattered by a portion of an elliptic cylinder which satisfies the equation

$$\frac{z^2}{a^2} + \frac{x^2}{a^2 - c^2} = 1 \quad , \tag{2}$$

as shown in Figure 1. We shall assume that the field point is located at P_2 and that the feed is a line source located at P_1 and radiating a magnetic field

$$\underline{H}_i = \hat{\theta}\, G(\theta)\, \frac{e^{-iku}}{u^{1/2}} \quad , \tag{3}$$

where $\hat{\theta}$ and $\hat{x} \cos\theta - \hat{z} \sin\theta$.

In order to evaluate Eq. (1), we shall find it convenient to write the integration in terms of the angle β which is defined in Figure 1. In terms of β, we find $dx = a\,\alpha^2 b^2 (\cos\beta - e)\, d\beta$, where $e = c/a$ = eccentricity, $b^2 = a^2 (1 - e^2)$ and $\alpha = a^{-1} (1 - e \cos\beta)^{-1}$. Also

$$\rho = [p^2 + \alpha^2 b^4 - 2p\alpha b^2 \cos(\eta - \beta)]^{1/2} \quad , \tag{4}$$

---

*provided $k\rho \gg 1$.

6. Silver, S. (1965) Microwave Antenna Theory and Design, Dover, New York.

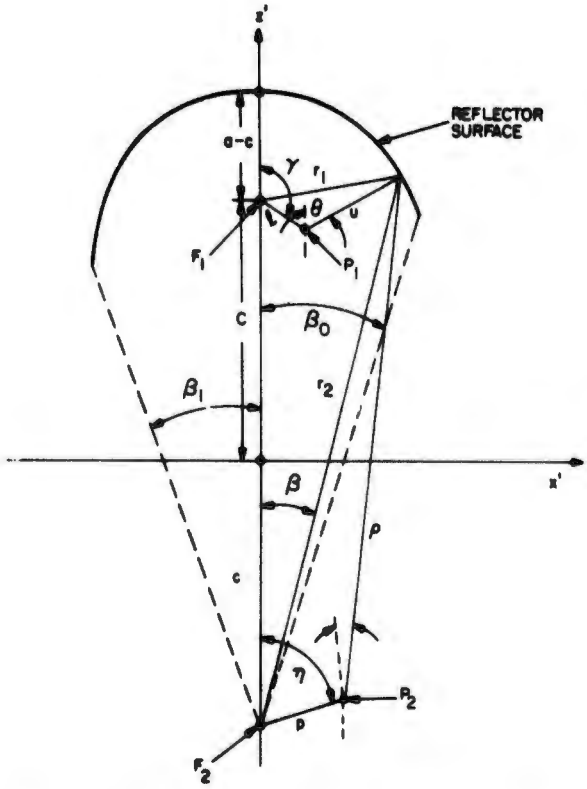

Figure 1. Elliptic Cylinder Reflector Geometry. Note that $r_1 + r_2 = 2a$

$$u = [\ell^2 + \alpha^2\tau^2 - 2\ell\alpha(s\cos\gamma + b^2\sin\beta\sin\gamma)]^{1/2} \quad , \tag{5}$$

where $\tau = a^2(1 - 2e\cos\beta + e^2)$ and $s = a^2(1 + e^2)\cos\beta - 2ea^2$. If we use Eqs. (4) and (5) in Eq. (1), along with the relations $x = b^2\alpha\sin\beta$, $z = b^2\alpha\cos\beta - c$, $x' = \rho\sin\eta$ and $z' = -c + \rho\cos\eta$, we get

$$H(P_2) = -\left(\frac{ik}{2\pi}\right)^{1/2} b^2 \int_{-\beta_1}^{\beta_0} d\beta\, F(\beta)\, e^{-ik(\rho+u)}$$

$$\cdot \{\hat{x}(\rho\cos\eta - \alpha b^2\cos\beta) - \hat{z}(\rho\sin\eta - \alpha b^2\sin\beta)\} \quad , \tag{6}$$

where

$$F(\beta) = \frac{\alpha^2 a(\cos\beta - e)G(\beta)}{(u\rho)^{3/2}} \left[\alpha s - \ell \cos\gamma + \frac{\alpha b^2 \sin^2\beta - \ell \sin\gamma \sin\beta}{|\cos\beta - e|} \right] . \quad (7)$$

Conversely, if the feed is a line source at P_2 radiating a magnetic field

$$\underline{H}_i = \hat{\xi}\, G_1(\xi) \frac{e^{-ik\rho}}{(\rho)^{1/2}} , \quad (8)$$

where $\hat{\xi} = \hat{x}\cos\xi - \hat{z}\sin\xi$ we can readily show that the magnetic field at P_1 is

$$\underline{H}(P_1) = -\left(\frac{ik}{2\pi}\right)^{1/2} b^2 \int_{-\beta_1}^{\beta_o} d\beta\, T(\beta)\, e^{-ik(\rho+u)} [\hat{x}(2c + \ell \cos\gamma - b^2 \alpha \cos\beta)$$

$$- \hat{z}(\ell \sin\gamma - b^2 \alpha \sin\beta)] , \quad (9)$$

where

$$T(\beta) = \frac{\alpha^2 a(\cos\beta - e)\, G_1(\beta)}{(u\rho)^{3/2}} \left\{ \alpha b^2 \cos\beta - p\cos\eta + \frac{\alpha b^2 \sin^2\beta - p \sin\eta \sin\beta}{|\cos\beta - e|} \right\} \quad (10)$$

and ξ and β are related via

$$\tan\xi = \frac{\alpha b^2 \sin\beta - p\sin\eta}{\alpha b^2 \cos\beta - p\cos\eta} . \quad (11)$$

2.2 Field at the Focus F_2

We now evaluate Eq. (6) for the field at the focus F_2 when the source is at F_1. If we assume that $\beta_o = \beta_1$ and that the feed is isotropic, we obtain

$$\underline{H}(F_2) = \hat{x} \left(\frac{1+e}{1-e}\right)^{1/2} A_1 \int_0^{\beta_o} \frac{d\beta \cos\beta}{\left[1 + \frac{4e}{(1-e)^2} \sin^2\left(\frac{\beta}{2}\right)\right]^{1/2}} , \quad (12)$$

where $A_1 = 2\,G(0)(ik/2\pi)^{1/2}$ exp (-i2ka) and e = c/a is the eccentricity of the ellipse. Equation (12) has been evaluated numerically for a number of different values of e and β_o; the results are presented in Figure 2. Note that the focal field no longer increases rapidly with increasing β_o once $\beta_o > 2 \sin^{-1} [(1 - e)/2e^{1/2}]$. Often it is convenient to know the relationship of the field strength to the angle Ψ_o subtended at the near focus, F_1, by the reflector edges. This can be done using Figure 3. Additionally, in Figure 4 we show the relationship between β_o and the reflector diameter d. By cross plotting the results in Figures 2 and 4, one can see that if d and the distance, a + c, from the reflector center to F_2 are held constant, then the field at F_2 is greatest when the eccentricity, e, is as large as possible.

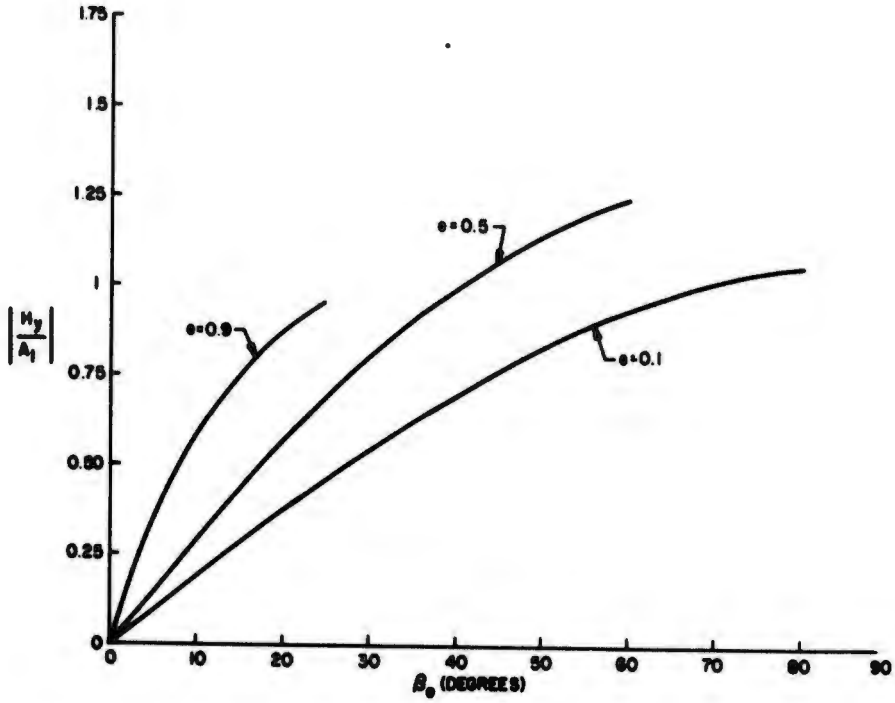

Figure 2. Magnitude of the Magnetic Field Produced at F_2 When an Elliptic Cylinder is Fed by an Isotropic Source at F_1. Note that $A_1 = 2\,G(0)(ik/2\pi)^{1/2}$ exp (-i2ka)

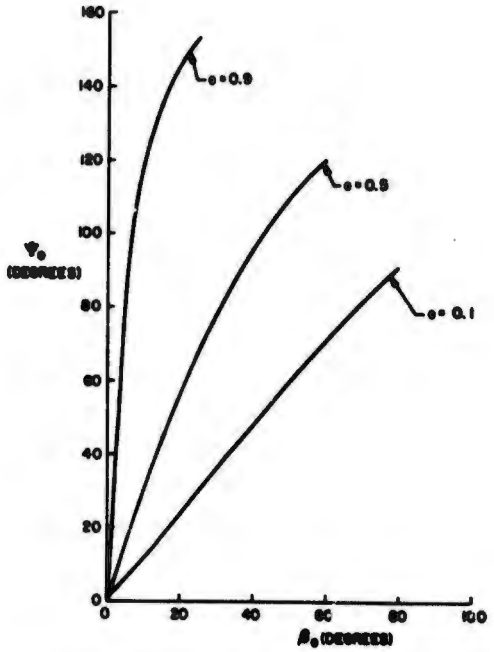

Figure 3. Relationship Between the Angle β_o Subtended by the Reflector Edge at F_2 and the Angle ψ_o Subtended by the Same Edge at F_1

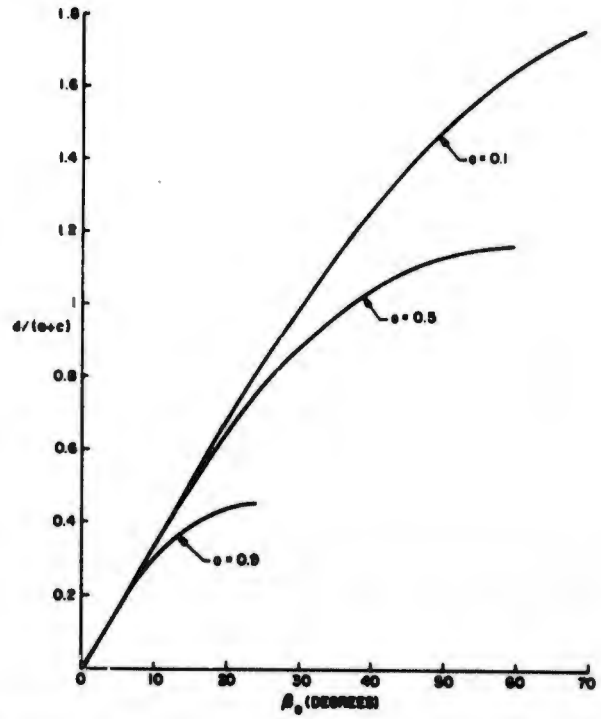

Figure 4. Relationship Between the Transverse Diameter of the Reflector and the Angle β_o Subtended by the Reflector Edge at F_2

2.3 Field Distribution Near F_2

It is very desirable to obtain analytical results for the field distribution in the volume around F_2. This can be accomplished if we assume that both β_o and β_1 are small in comparison with unity. Of course this does not imply that the angle, Ψ_o, subtended at F_1 by the reflector edges is also small, as is evident from a glance at Figure 3. If we require that $\beta_o \ll 1$, $\beta_1 \ll 1$, $e\beta_o^2/(1-e)^2 < 1$ and $e\beta_1^2/(1-e)^2 < 1$, it is possible to demonstrate that Eq. (6) can be rewritten as

$$\underline{H}(P_2) = A \int_{-\beta_1}^{\beta_o} d\beta\, G(\beta) \left[\hat{x}\left(1 - \frac{p\cos\eta}{a+c}\right) + \hat{z}\left(\frac{p\sin\eta}{a+c} - \beta\right)\right]$$

$$\cdot \exp\{ik[2c_1\beta - c_2\beta^2 + o(\beta^3)]\} \quad , \tag{13}$$

where

$$A = (ik/2\pi)^{1/2}[(1+e)/(1-e)]^{1/2} \exp\{-ik(M^{1/2} + N^{1/2})\} \quad ,$$

and

$$c_1 = \frac{a(1+e)}{2}\left[\frac{p\sin\eta}{M^{1/2}} + \frac{\ell\sin\gamma}{N^{1/2}}\right] \tag{14}$$

$$c_2 = -\frac{a(1+e)}{2}\left[\frac{ae(1+e)}{(1-e)M^{1/2}} + \frac{a(1+e)p^2\sin^2\eta}{M^{3/2}} - \frac{p\cos\eta}{(1-e)M^{1/2}}\right.$$

$$\left. - \frac{ae}{N^{1/2}} - \frac{\ell\cos\gamma}{(1-e)N^{1/2}} + \frac{a(1+e)\ell^2\sin^2\gamma}{N^{3/2}}\right] \quad , \tag{15}$$

$M = p^2 + a^2(1+e)^2 - 2a(1+e)\,p\cos\eta$ and $N = \ell^2 + a^2(1-e)^2 - 2a(1-e)\,\ell\cos\gamma$. Instead of using polar coordinates, we could also have written Eq. (13) in terms of the rectangular coordinates $x_2 = p\sin\eta$, $z_2 = p\cos\eta$, $x_1 = \ell\sin\gamma$, $z_1 = \ell\cos\gamma$. In writing Eqs. (13) to (15), we have also implicitly assumed that $p \le a(1+e)$ and $\ell \le a(1-e)$.

In Eq. (13) the term of order β^3 in the exponent can be neglected if $p/\lambda < \beta_o^{-3}$ and $\ell/\lambda < \beta_o^{-3}(1-e)/(1+e)$ where λ is the signal wavelength. If we assume that $G(\beta)$ is isotropic and that p and ℓ satisfy the above conditions, so that the β^3 term in the exponent can be ignored, we can evaluate Eq. (13) as

$$H_x(P_2) = A\,G(0)\left[1 - \frac{p\cos\eta}{a+c}\right]Q(p, \underline{\ell}) \quad , \tag{16}$$

$$H_z(P_2) = A\,G(0)\left\{Q(p, \underline{\ell})\left[\frac{p\sin\eta}{a+c} - \frac{c_1}{c_2}\right] + (2ikc_2)^{-1}\right.$$

$$\left.\left[e^{-ikc_2(\beta_o - c_1/c_2)^2} - e^{-ikc_2(\beta_1 + c_1/c_2)^2}\right]\right\} \quad , \tag{17}$$

where

$$Q = \gamma^{-1}\left\{C\left[\gamma\left(\beta_o - \frac{c_1}{c_2}\right)\right] + C\left[\gamma\left(\beta_1 + \frac{c_1}{c_2}\right)\right] - i\,S\left[\gamma\left(\beta_o - \frac{c_1}{c_2}\right)\right]\right.$$

$$\left. - i\,S\left[\gamma\left(\beta_1 + \frac{c_1}{c_2}\right)\right]\right\} \quad , \tag{18}$$

$\gamma = (2kc_2/\pi)^{1/2}$ and C(v) and S(v) are the Fresnel integrals, defined in Ref. 7. Equations (16) and (17) give the complete field distribution near F_2 for arbitrary source displacements ℓ, provided p, ℓ, β_o and β_1 satisfy the restrictions discussed previously.

By studying Eqs. (16) and (17), or by applying the Schwartz inequality directly to Eq. (13), we can see that the peak field magnitude occurs at the point where $c_1 = c_2 = 0$. Thus as the source is moved away from F_1, the center of the focal spot will move to a position such that $c_1 = c_2 = 0$. By setting $c_1 = 0$ in Eq. (14) and $c_2 = 0$ in Eq. (15), we find that the coordinates, $x_2 = p\sin\eta$ and $z_2 = p\cos\eta$, of the center of the focal spot are

$$z_2 = -a(1+e)\left[\frac{e}{1-e} + K^2 - \frac{M_o}{(1-K^2)^{1/2}}\right]\left[\frac{M_o}{(1-K^2)^{1/2}} - \frac{1}{(1-e)}\right]^{-1} \quad , \tag{19}$$

$$x_2 = -\frac{a(1+e)K}{(1-K^2)^{1/2}}\left[1 - \frac{z_2}{a(1+e)}\right] \quad . \tag{20}$$

where $K = \ell N^{-1/2} \sin\gamma$ and $M_o = eaN^{-1/2} + \ell \cos\gamma(1+e)^{-1} N^{-1/2} - \ell^2 a(1+e) N^{-3/2} \sin^2\gamma$. As an example of the motion of the focus, let us suppose that $\gamma = -\pi/2$ so that the source is displaced from F_1 along a straight line transverse to the z-axis. In this case Eqs. (18) and (19) become $z_2 = 2at^2(1+e)[(1-e)^3 + 2t^2]^{-1}$ and $x_2 = -at[(1+e)/(1-e)][1 + 2t^2/(1-e)^3]^{-1}$, where $t = \ell/a$. A plot of the motion of the center of the focal spot is shown in Figure 5, for the cases when $e = 0.8, 0.9$. Consequently, the deflection of the feed along a straight line in the x direction produces a nearly parabolic locus for the motion of the focal spot.

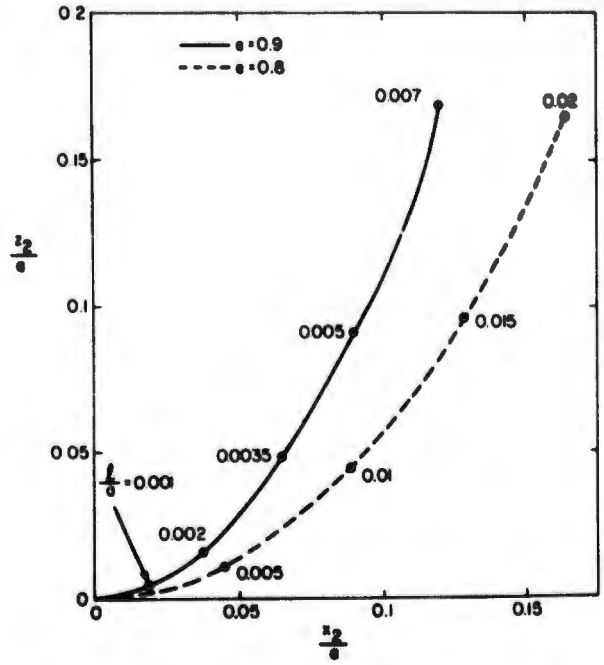

Figure 5. Locus Followed by the Center of the Focal Spot When the Feed is Displaced along a Straight Line Transverse to the z-Axis ($\gamma = -\pi/2$)

When β_o is no longer small or the source displacement ℓ/λ exceeds $\beta_o^{-3}(1-e)/(1+e)$, the results in Eqs. (16) to (20) are no longer adequate. In this case, it is necessary to retain higher order terms in β in Eq. (13), and this results in a smearing out of the focal region, with Eqs. (19) and (20) representing an increasingly poorer approximation to the location of the center of the spot.

Now that we have studied the motion of the spot for relatively large displacements of the feed, let us examine Eqs. (16) and (17) in the limit when the

displacement of the feed from F_1 is very small. We shall assume that the reflector is symmetric ($\beta_o = \beta_1$) and the displacements p and ℓ are transverse to the z-axis. If we set $\gamma = -\pi/2$ (see Figure 6), we find for the field distribution in the F_2 plane ($\eta = \pi/2$)

$$\underline{H}(P_2) = 2\beta_o A\, G(0) \left[\hat{x} + \hat{z}\, \frac{p}{a+c}\right] \operatorname{sinc}\left\{k\beta_o \left[p - \ell\left(\frac{1+e}{1-e}\right)\right]\right\} , \tag{21}$$

where sinc(y) = siny/y. We observe from Eq. (21) that if the feed is displaced by a transverse distance $\ell \ll (a - c)$, the center of the focal spot is displaced by a transverse distance

$$p = \left(\frac{1+e}{1-e}\right)\ell \quad . \tag{22}$$

In addition, we find that the transverse dimension of the focal spot is

$$\Delta p \simeq \pm \frac{\lambda}{2\beta_o} \quad . \tag{23}$$

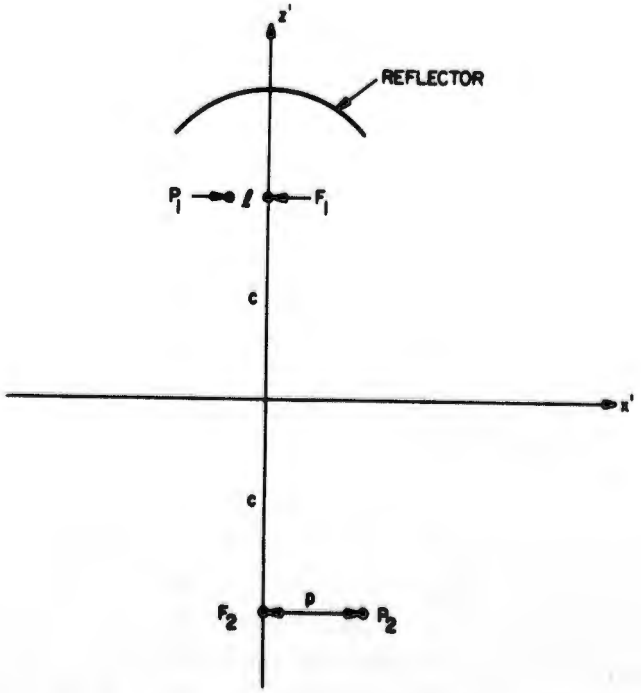

Figure 6. Transverse Displacement of the Focal Point Produced by a Transverse Displacement of the Feed Point

We can next turn our attention to the field distribution along the z-axis. If we set $\gamma = \pi$ and $\eta = o$, so that the source is located at P_1 and the field point is at P_2, as shown in Figure 7, we find

$$\underline{H}(P_2) = \hat{x}\, 2G(0)\, A\, e^{-ik(2a-p-\ell)} \left(\frac{\pi}{\Lambda}\right)^{1/2} \left\{ C\left[\beta_o \left(\frac{\Lambda}{\pi}\right)^{1/2}\right] - iS\left[\beta_o \left(\frac{\Lambda}{\pi}\right)^{1/2}\right]\right\} , \tag{24}$$

where

$$\Lambda = k\left[p - \ell\left(\frac{1+e}{1-e}\right)^2\right] . \tag{25}$$

From Eqs. (24) and (25) it is clear that if the source is axially displaced from F_1 by a distance $\ell \ll (a - c)$, the center of the focal spot is displaced from F_2 by

$$p = \ell\left(\frac{1+e}{1-e}\right)^2 \tag{26}$$

provided* $p \ll (a + c)$. The depth of focus is determined by finding the values of p at which $|\underline{H}|^2$ is equal to one half of its value when p is given by Eq. (26). We find that this occurs when $\beta_o(\Lambda/\pi)^{1/2} = 1.3$. Therefore the depth of focus is

$$\delta p = \pm \frac{1.69\,\pi}{k\,\beta_o^2} \tag{27}$$

provided $|\delta_p| \ll (a + c)$.

Before leaving this section, one finds it interesting to note that if the source is at P_2 and the field point is at P_1, we find that the transverse distribution is still given by Eq. (21), except with G(0) replaced by $G_1(0)$ and $[\hat{x} + \hat{z}\, p/(a + c)]$ replaced by $[\hat{x} - \hat{z}\, \ell/(a - c)]$. The field along the z-axis is again given by Eq. (24), except with G(0) replaced by $G_1(0)$. Therefore, a transverse displacement p of the source now produces a transverse displacement of the focal spot $\ell = [(1 - e)/(1 + e)]p$, and the transverse dimension of the focal spot is $\Delta\ell = \pm (\lambda/2\beta_o)[(1 - e)/(1 + e)]$.

---

*For larger values of ℓ and p we find for the displacement:

$$p = \ell\left(\frac{1+e}{1-e}\right)^2 \left[1 + \frac{2\ell}{a(1-e)^2}\right]^{-1}$$

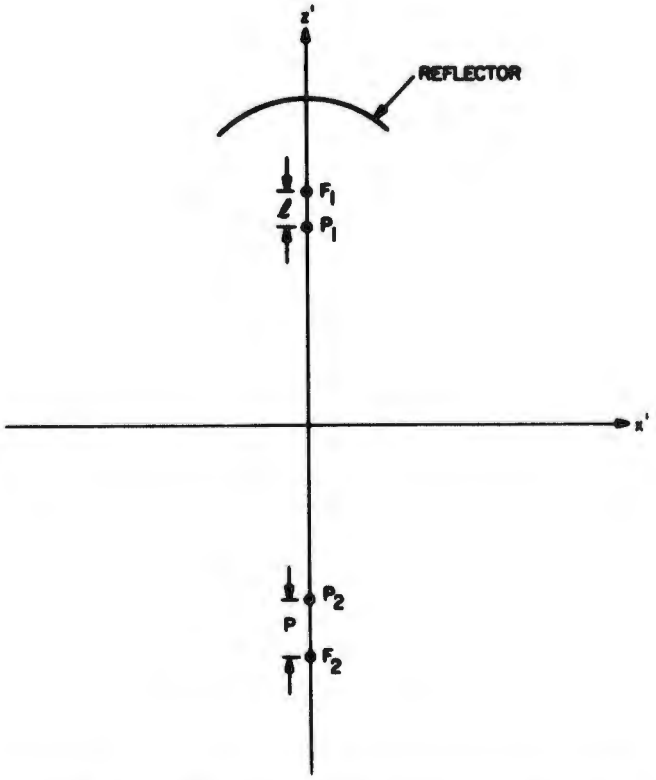

Figure 7. Longitudinal Displacement of the Focal Point Produced by a Longitudinal Displacement of the Feed Point

2.4 Field at Points Distant from the Foci

The analysis in Section 3 is appropriate for calculating the field near F_2 (or F_1), but fails when p or ℓ is very large. When the transverse dimension of the reflector is large compared with the wavelength and $k(\rho + u - 2a) \gg 1$ the field at P_2 can be calculated by the method of stationary phase. In that case Eq. (6), or Eq. (9), can be evaluated as the sum of a stationary point contribution plus the sum of the contributions from the two end points ($\beta = -\beta_1$ and $\beta = \beta_0$) of the reflector. Note that, in this section, β_0 and β_1 are <u>not</u> assumed to be small.

The stationary point in the integration in Eq. (6) occurs at the value or values of β at which $d/d\beta(\rho + u) = 0$. Upon using Eqs. (4) and (5) for ρ and u, we find that the stationary point satisfies

$$h(\beta) \equiv \alpha^2 b^2 \left\{ \frac{-b^2 c \alpha \sin\beta + p[a \sin(\beta - \eta) + c \sin\eta]}{\rho} \right.$$

$$\left. + \frac{c \alpha \tau \sin\beta + \ell[a \sin(\beta - \gamma) + c \sin\gamma]}{u} \right\} = 0 \quad , \tag{28}$$

where $h(\beta) = d(u + \rho)/d\beta$. In order to keep our calculations tractable, we shall now assume that $\ell \ll (a - c)$, but will allow β_o, β_1 and p to remain arbitrary. This means that we will assume that the source lies near F_1, but that the observation point is arbitrary, provided p is sufficiently large that $kp \gg 1$ and $p \gg [(1 + e)/(1 - e)]\ell$. When the aforementioned conditions are satisfied, we find that the stationary points in the range $-\pi/2 \le \beta \le \pi/2$ are located approximately at $\beta_s \simeq -\eta$ whenever $-\pi/2 < \eta < \pi/2$. However, when $\pi/2 < \eta < \pi$, we find that the stationary point lies at $\beta_s = -(\pi - \eta)$, and for $-\pi/2 > \eta > -\pi$, we find that $\beta_s \simeq \pi + \eta$.

Once the location of the stationary point is known, we can readily obtain the asymptotic evaluation of the integral in Eq. (6) using standard techniques.[8] The result is (provided $\beta_s \neq \beta_o$, $\beta_s \neq -\beta_1$)

$$\underline{H}(P_2) = \left| \frac{2\pi}{k q(\beta_s)} \right|^{1/2} \underline{W}(\beta_s)\, e^{\mp i\pi/4}\, u_{-1}[(\beta_s + \beta_1)(\beta_o - \beta_s)]$$

$$+ \frac{\underline{W}(\beta_o)}{-ikh(\beta_o)} - \frac{\underline{W}(-\beta_1)}{ikh(-\beta_1)} \quad , \tag{29}$$

where $u_{-1}(\ldots)$ is the unit step function, β_s is the stationary point discussed in the last paragraph, $h(\beta)$ is defined in Eq. (28), $q(\beta) = dh/d\beta$ and

$$\underline{W}(\beta) = -\left(\frac{ik}{2\pi}\right)^{1/2} b^2 F(\beta) \{\hat{x}(p \cos\eta - \alpha b^2 \cos\beta) - \hat{z}(p \sin\eta - \alpha b^2 \sin\beta)\}$$

$$\exp\{ik[\rho(\beta) + u(\beta)]\} \quad . \tag{30}$$

The upper signs in Eq. (29) are used if $q > 0$ and the lower ones if $q < 0$. Some sample plots of the asymptotic field distribution, as approximated by Eq. (29), are shown in Figures 8 and 9 for the case when the feed is isotropic and located at F_1.

---

8. Felsen, L., and Marcuvitz, N. (1973) Radiation and Scattering of Waves, Prentice Hall, New York.

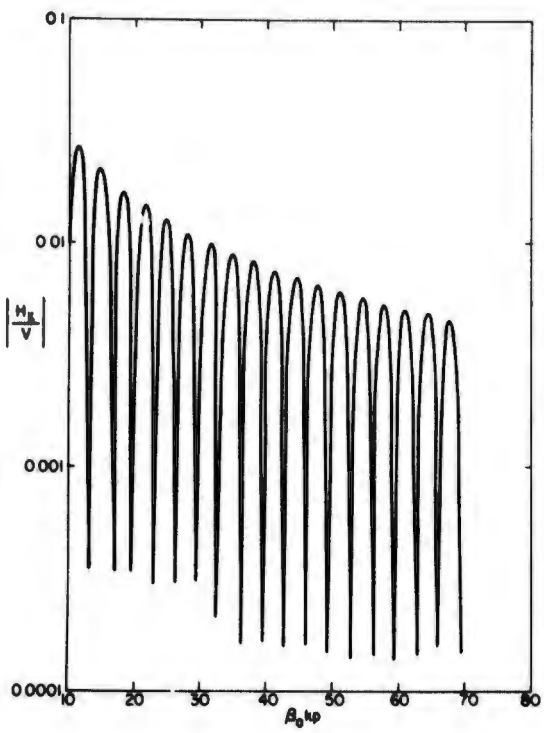

Figure 8. X-component of the Asymptotic H-field in the Transverse Plane Passing through $F_2(\eta = \pi/2)$, for the Case when $\ell = 0$, $\beta_o = 30^o$ and $e = 0.5$. Calculated using Eq. (29). $V = b^2 G(0) (2\pi k)^{-1/2}$

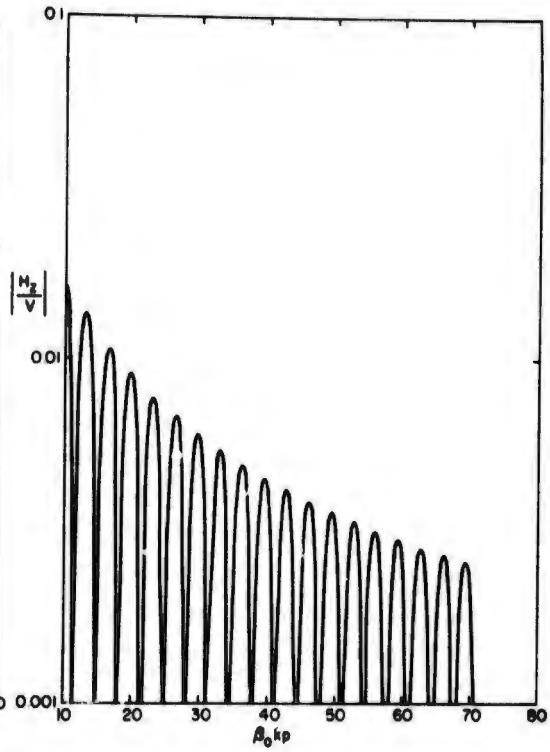

Figure 9. Z-component of the Asymptotic H-field in the Transverse Plane Passing through $F_2(\eta = \pi/2$, for the Case when $\ell = 0$, $\beta_o = 30^o$ and $e = 0.5$. Calculated using Eq. (29). $V = b^2 G(0) (2\pi k)^{-1/2}$

We have shown that these results are a good approximation to the field distribution calculated directly from Eq. (6).

The first term in Eq. (29) represents the contribution to the field due to the stationary point, whereas the last two terms represent the contributions from the end points of the reflector. From this result and our studies in the last section, it is clear that:

1. The field near the foci is produced by currents over the entire reflector.

2. At points many wavelengths from the foci, the field is composed of contributions from the edges of the reflector, plus a contribution from a stationary point. This contribution from the stationary point may or may not be present, depending on the relative sizes of η, β_o and β_1.

These conclusions are illustrated in Figure 10, for the case when $\ell = 0$. Note that there is a region where both the stationary point and the end points contribute to the field, and another where the field is due only to the end point contributions.

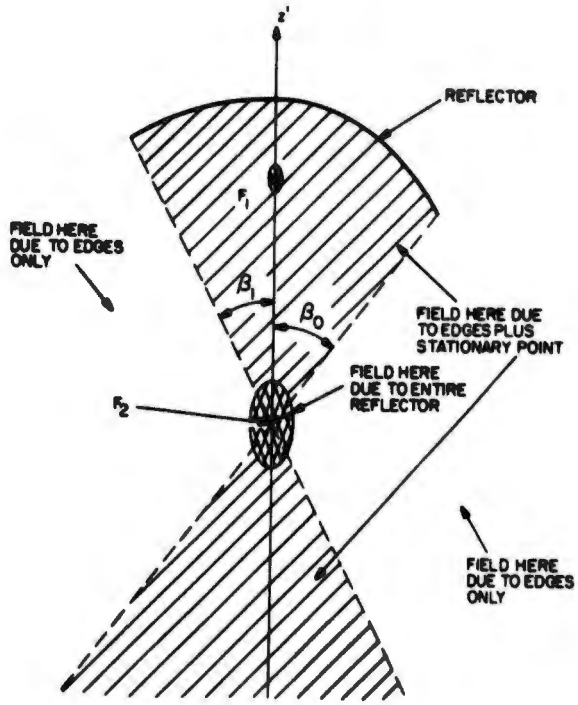

Figure 10. Pictorial Illustration of Portions of the Reflector Which Contribute to the Field at a Given Point

It is interesting to compare the result in Eq. (29) with results in Section 3, for the case when $\beta_o = \beta_1$, $\beta_o \ll 1$ and $p \ll (a + c)$. In this limit we find from Eq. (29) that for $\eta = \pi/2$, so that $\beta_s = \pm \pi/2$, the first term in Eq. (29) vanishes and the only contributions are from the last two terms in Eq. (29). These are found to reduce identically to Eq. (21) in this limit.

Next we consider the case when $\eta = 0$ or π so that the field point lies on the z-axis (but not, of course, too close to F_2). In this case there is a stationary point at $\beta_s = 0$ and the first term in Eq. (29) does not vanish. Now Eq. (29) reduces to

$$\underline{H}(P_2) = \hat{x}\, e^{i(\pi/4 \mp \pi/4)} \frac{G(0)}{p^{1/2}} \left(\frac{1+e}{1-e}\right)^{1/2} e^{-ik(2a \mp p)} \mp \hat{x}\, 2\, e^{-i\pi/4} \left(\frac{1}{2\pi k}\right)^{1/2}$$

$$\left[\frac{G(\beta_o) + G(-\beta_o)}{2\beta_o p}\right]^{1/2} \left(\frac{1+e}{1-e}\right)^{1/2} e^{-ik(2a \mp p \pm \beta_o^2/2p)} \,. \qquad (31)$$

where the upper signs in Ec. (31) are for $\eta = 0$ and the lower ones for $\eta = \pi$. Also, in deriving Eq. (31), we have set $\ell = 0$ and again assumed $\beta_o = \beta_1 \ll 1$, $p \ll (a + c)$. When $G(\beta)$ is independent of β over the range $-\beta_o \le \beta \le \beta_o$, it is easily shown that Eq. (31) is identical with the asymptotic limit of Eq. (24). Of course, Eq. (31) cannot agree with Eq. (24) for small p, because in that case the method of stationary phase is inappropriate.

2.5 Field in the Shadow Region

We shall now examine the validity of Eq. (29) in the shadow region behind the reflector (see Figure 11). In the shadow region the first term in Eq. (29) is not present, and the diffraction field is given solely by the edge contributions, so that

$$\underline{H}(P_2) = \frac{W(\beta_o)}{-ikh(\beta_o)} - \frac{W(-\beta_1)}{-ikh(-\beta_1)} \quad . \tag{32}$$

If we evaluate Eq. (32) for $\ell = 0$ and $p \to \infty$ we find that

$$\underline{H}(P_2) = \hat{\eta}\,[D_p(\beta_o)\,H_i(\beta_o) - D_p(\beta_1)\,H_i(-\beta_1)]\,\frac{e^{-ikp}}{p^{1/2}} \quad , \tag{33}$$

where $\hat{\eta} = \hat{x}\cos\eta - \hat{z}\sin\eta$, $H_i(\beta) = G(\beta)u^{-1/2}\exp(-iku)$ and the physical-optics diffraction coefficient is

$$D_p(\beta) = \left(\frac{1}{2\pi k}\right)^{1/2} \frac{(\cos\beta - e)\left[\varepsilon + \dfrac{b^2\sin^2\beta}{|\cos\beta - e|}\right] e^{i\pi/4}}{|\sin(\beta - \eta) + e\sin\eta + e\sin\beta|\tau} \quad . \tag{34}$$

It is now desirable to compare this diffraction coefficient with the diffraction coefficient computed via the geometrical theory of diffraction. If we assume the field point is at P_0 on the z-axis, as shown in Figure 11, it can be shown[9] that the geometrical theory of diffraction yields for the diffraction coefficient at the edge $\theta = \theta_o$ (see Figure 11)

---

9. James, G., and Kerdemelidas, V. (1973) Reflector antenna radiation pattern analyzed by equivalent edge currents, IEEE Trans. Ant. Prop. 21:19-24.

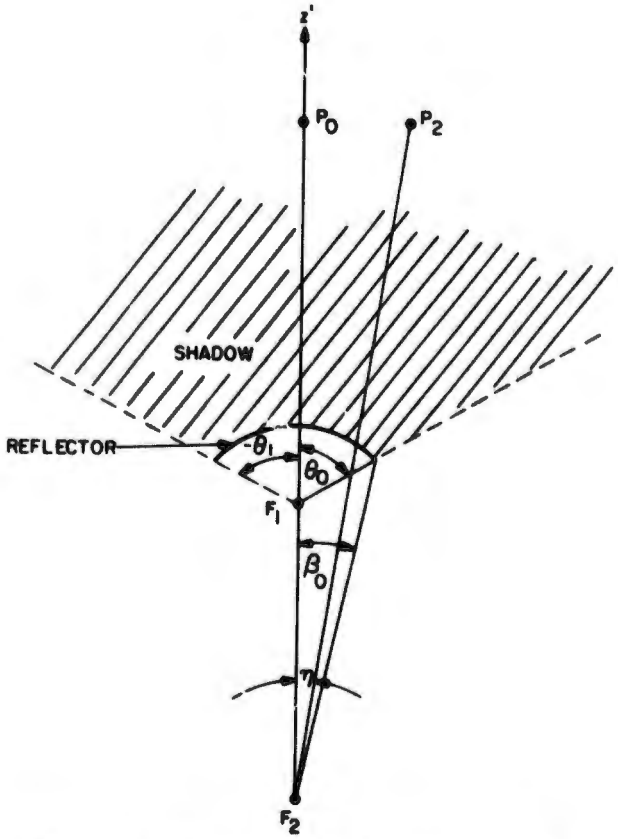

Figure 11. Geometry for Consideration of the Field in the Shadow Region

$$D_g = \frac{e^{-i\pi/4}\left[1 - \sin\left(\frac{\theta_0}{2}\right)\right]}{2(2\pi k)^{1/2}\sin\left(\frac{\theta_0}{2}\right)} \cdot , \tag{35}$$

where θ_0 can be related to β_0 via

$$\sin\left(\frac{\theta_0}{2}\right) = \sin\left(\frac{\beta_0}{2}\right)\frac{1+e}{[1+e^2-2e\cos\beta]^{1/2}} \cdot \tag{36}$$

We now use Eq. (36) in Eq. (35) and then take the ratio of D_p to D_g. In the limit when $\beta_0 \ll 1$ we get

$$\frac{D_p}{D_g} = \frac{1 + \frac{(1+e)}{(1-e)^2}\beta_o^2}{1 - \left(\frac{1+e}{1-e}\right)\frac{\beta_o}{2}} \quad . \tag{37}$$

From Eq. (37) it is clear that if $\beta_o \ll (1 - e)/(1 + e)$, the physical-optics diffraction coefficient is approximately equal to the diffraction coefficient computed using the geometrical theory of diffraction. However for $\beta_o \gtrsim (1 - e)/(1 + e)$ the physical theory of diffraction no longer gives results equivalent to those obtained by the geometrical theory of diffraction. For example, if $\beta_o = 30^o$, a = 5 and c = 2 we get from Eqs. (34) and (35) that $D_p/D_g = 2.1$.

Therefore, when $\beta_o \ll (1 - e)/(1 + e)$ we may use Eq. (32) to calculate the field in the shadow region, provided P_2 does not lie on or too near to the shadow boundary. When $\beta_o > (1 - e)/(1 + e)$, it is necessary to employ the geometrical theory of diffraction to calculate the field in the shadow, although Eq. (32) still gives a "ballpark" estimate even in this case.

2.6 A Comment on Other Reflector Shapes

It is interesting to note that the same conclusions we have reached in Sections 4 and 5 also hold[10, 11] for other reflector shapes, including those which have their second focus, F_2, at infinity. For example, we have also studied the offset parabolic cylinder shown in Figure 12. For this case, the region corresponding to the focal region around F_2 in Figure 10 now maps into the main beam of the antenna, and the region shown in Figure 10 as outside the focal spot now maps into the sidelobes of the radiation field. For the offset parabolic cylinder, there is no stationary point within the integration range and the far-field sidelobes are due solely to the reflector edge contributions. For example, when the feed is located at F_1 and emits a field given by Eq. (3) we find that the sidelobe radiation field from a large (in wavelengths) offset parabolic cylinder is

$$\underline{H}(P_2) = \underline{V}(\theta_o) - \underline{V}(\theta_1) \quad . \tag{38}$$

---

10. Knop, C. (1976) On the front to back ratio of a parabolic dish antenna, IEEE Trans. Ant. Prop. 24:109-111.
11. Rusch, W. (1974) Antenna Notes, Vol II, NB. 846, Tech Univ., Lyngby, Denmark, 135-141.

where

$$\underline{V}(\theta) = \frac{\hat{\psi}\, e^{-i\pi/4}\, G(\theta) \left(1 + \tan^2 \frac{\theta}{2}\right)^{1/2} \exp\{-ik(R_o + F_1)\}}{(2\pi k F_1 R_o)^{1/2} \sin\psi [1 - 2 \tan\frac{\theta}{2} \sin^2 \frac{\psi}{2} \sin^{-1}\psi]}$$

$$\cdot \exp\left\{i 2 k F_1 \sin\psi \tan\frac{\theta}{2} \left(1 - \tan\frac{\theta}{2} \sin^2 \frac{\psi}{2} \sin^{-1}\psi\right)\right\} \quad , \tag{39}$$

where $\hat{\psi}$ is a unit vector defined as $\hat{\psi} = \hat{x} \cos\psi + \hat{z} \sin\psi$. Equation (38) is valid provided ψ is sufficiently large that $|2 k F_1 \sin\psi| \gg 1$. The result in Eq. (38) agrees quite well with exact computer calculations we have performed for the side-lobe fields.

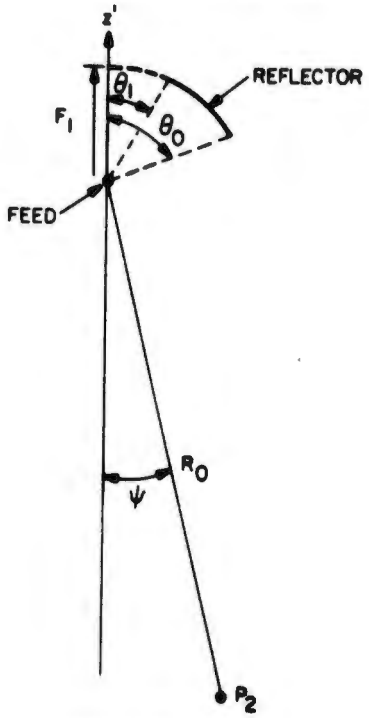

Figure 12. Offset Parabolic Cylinder Reflector

3. ELLIPSOID OF REVOLUTION

3.1 Analytical Formalism

The magnetic field scattered by a reflector with a surface satisfying the equation $z = f(x, y)$ can be written, in the physical optics approximation, as

$$\underline{H}(x', y', z') = \frac{ik}{2\pi} \iint_{S_o} \frac{dx\, dy}{\rho} \left\{ \left(\hat{z} - \hat{x} \frac{\partial f}{\partial x} - \hat{y} \frac{\partial f}{\partial y} \right) \times \underline{H}_i \right\}$$

$$\times \{(x' - x)\, \hat{x} + (y' - y)\, \hat{y} + (z' - z)\, \hat{z}\} \frac{e^{-ik\rho}}{\rho} \tag{40}$$

provided $k\rho \gg 1$. In Eq. (40), ρ is the distance from the field point (x', y', z') to the point (x, y, z) on the reflector, S_o is the projection of the reflector onto the x-y plane and $\underline{H}_i$ is again the magnetic field of the feed. We now assume that the reflector is an ellipsoid of revolution satisfying the equation*

$$\frac{z^2}{a^2} + \frac{x^2 + y^2}{a^2 - c^2} = 1 \tag{41}$$

and that the source lies at the point P_1 in Figure 13 and radiates the magnetic field

$$\underline{H}_i = \hat{\xi}\, G(\beta, \phi) \frac{e^{-iku}}{u} \quad , \tag{42}$$

where $\hat{\xi}$ is a unit azimuthal vector lying in the plane normal to the x-axis. When P_1 is close to F_1, we can write $\hat{\xi}$ in terms of the angles β and ϕ defined in Figure 13 as $\hat{\xi} \simeq D(\hat{y} \cos\beta - \hat{z} \sin\beta \sin\phi)$ where $D \equiv (\cos^2\beta + \sin^2\beta \sin^2\phi)^{-1/2}$. We further assume that the field point is at P_2 and has coordinates $x' = p \sin\eta \cos\phi_2$, $y' = p \sin\eta \sin\phi_2$ and $z' = p \cos\eta - c$. If we then express the integral in Eq. (40) in terms of the angles β and ϕ shown in Figure 13, we get

---

*We may also write Eq. (41) as $r_1 + r_2 = 2a$, where r_1 and r_2 are shown on Figure 13.

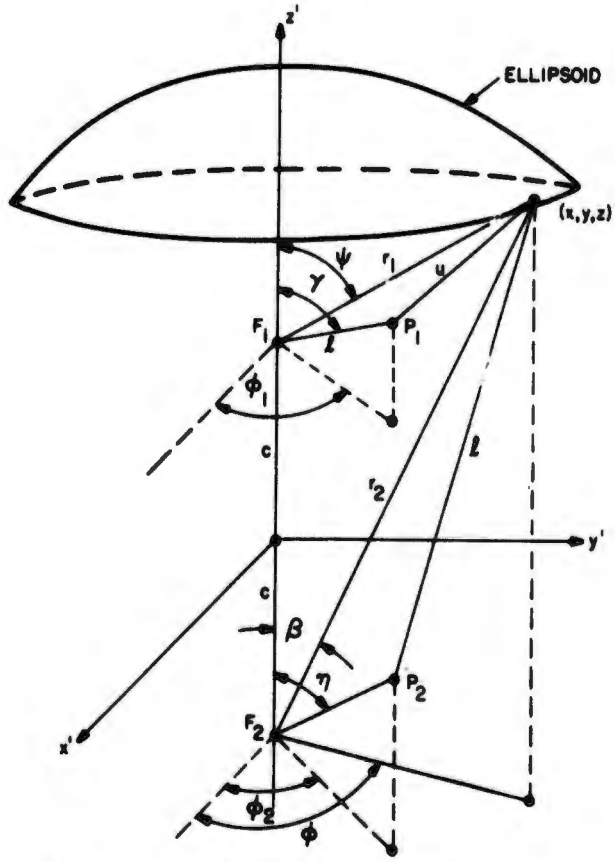

Figure 13. Ellipsoid of Revolution

$$\underline{H}(P_2) = \frac{ikb^4}{2\pi} \int_0^{\beta_0} d\beta \int_0^{2\pi} \frac{d\phi}{\rho^2 u} e^{-ik(\rho+u)} \{\hat{x}\,\gamma_2 [(z' - z)\sin\beta\sin\phi$$

$$- (y' - y)\cos\beta] + \hat{y}[\gamma_1(z' - z) + \gamma_2(x' - x)\cos\beta]$$

$$- \hat{z}[\gamma_1(y' - y) + \gamma_2(x' - x)\sin\beta\sin\phi]\}G(\beta,\phi) \quad , \tag{43}$$

where

$$\rho = [r_2^2 + p^2 - 2pr_2\{\sin\beta\sin\eta\cos(\phi - \phi_2) + \cos\eta\cos\beta\}]^{1/2} \quad , \tag{44}$$

$$u = [a^2\tau^2 + \ell^2 - 2a\ell\{s\cos\gamma + b^2\sin\beta\sin\gamma\cos(\phi - \phi_1)\}]^{1/2} \quad , \tag{45}$$

$$\gamma_1 = \frac{D}{a^2}\left[\frac{\sin^2\beta\sin^2\phi}{|\cos\beta - e|} + \cos\beta\right]\left[\frac{(\cos\beta - e)\sin\beta}{(1 - e\cos\beta)^3}\right] \quad , \tag{46}$$

$$\gamma_2 = \frac{D(\cos\beta - e)\sin^2\beta\cos\phi}{a^2|\cos\beta - e|(1 - e\cos\beta)^3} \quad , \tag{47}$$

Note that $r_2 = \alpha a(1 - e^2)$, $x = \alpha b^2 \sin\beta\cos\phi$, $y = \alpha b^2 \sin\beta\sin\phi$, $z = b^2\alpha\cos\beta - c$, α, s, b^2, τ were defined previously in Section A1, and β_o is the angle subtended at F_2 by the edge of the reflector.

3.2 Field Distribution Along the z-Axis

We can now compute the field distribution along the z-axis. If we assume that the feed is an isotropic source at F_1, and then analytically perform the ϕ-integration in Eq. (43) and numerically evaluate the β integration, we get the results shown in Figures 14 and 15, for the case when $\eta = \pi$. We note that for small eccentricities, the field structure along the axis behaves nearly like a sinc function, but as $e \to 1$ the structure deviates considerably from this. In addition, by comparing Figures 14 and 15, we note that the depth of the focal region is approximately proportional to β_o^{-2}.

When the source is at F_1 and p lies on the z-axis and is relatively close to F_2 (that is, $p \ll r_2$), the expression in Eq. (43) simplifies to the result

$$H_y(P_2) = -A_o\left(\frac{1+e}{1-e}\right)\int_0^{\beta_o} \frac{d\beta\sin 2\beta\, e^{\mp ikp\cos\beta}}{1 + \frac{4e}{(1-e)^2}\sin^2\left(\frac{\beta}{2}\right)} \quad , \tag{48}$$

where $e = c/a$, the upper sign applies to $\eta = \pi$ and the lower one to $\eta = 0$ and

$$A_o = \frac{ik}{2}\, G(0)\exp(i2ka) \quad . \tag{49}$$

From Eq. (48), it is clear that the field near the focus will be independent of the eccentricity if $4e(1 - e)^{-2}\sin^2(\beta_o/2) \ll 1$. Therefore, in agreement with Figures 14 and 15 the field distribution is nearly independent of the eccentricity for small values of e. In deriving Eq. (48), we have assumed that $e \leq \cos\beta_o$.

Equation (48) can also be used to calculate the effect of e and β_o on the focal field strength. If we set $p = 0$ and evaluate Eq. (48) we obtain the results shown

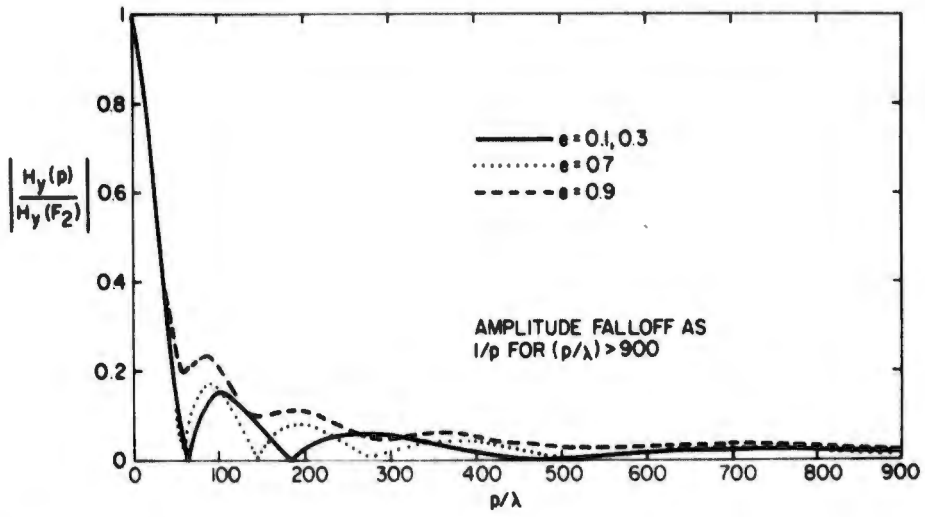

Figure 14. Magnetic Field Distribution along the z-Axis ($\eta = \pi$) for $\beta_o = 11.4^o$, and ka = 1256

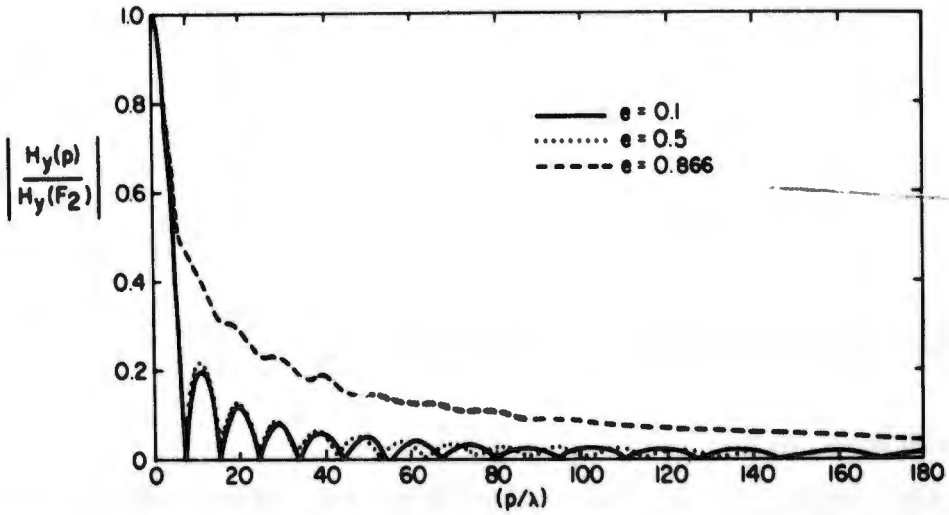

Figure 15. Magnetic Field Distribution along the z-Axis ($\eta = \pi$) for $\beta_o = 30^o$, and ka = 1256

in Figure 16. Note the break point at $\beta_o \simeq (1 - e)\, e^{-1/2}$ beyond which the field no longer increases rapidly with increasing β_o. As before, we can use Figures 3 and 4 to relate H to either the angle, Ψ_o, subtended by the rim of the reflector or to the diameter, d, of the reflector.

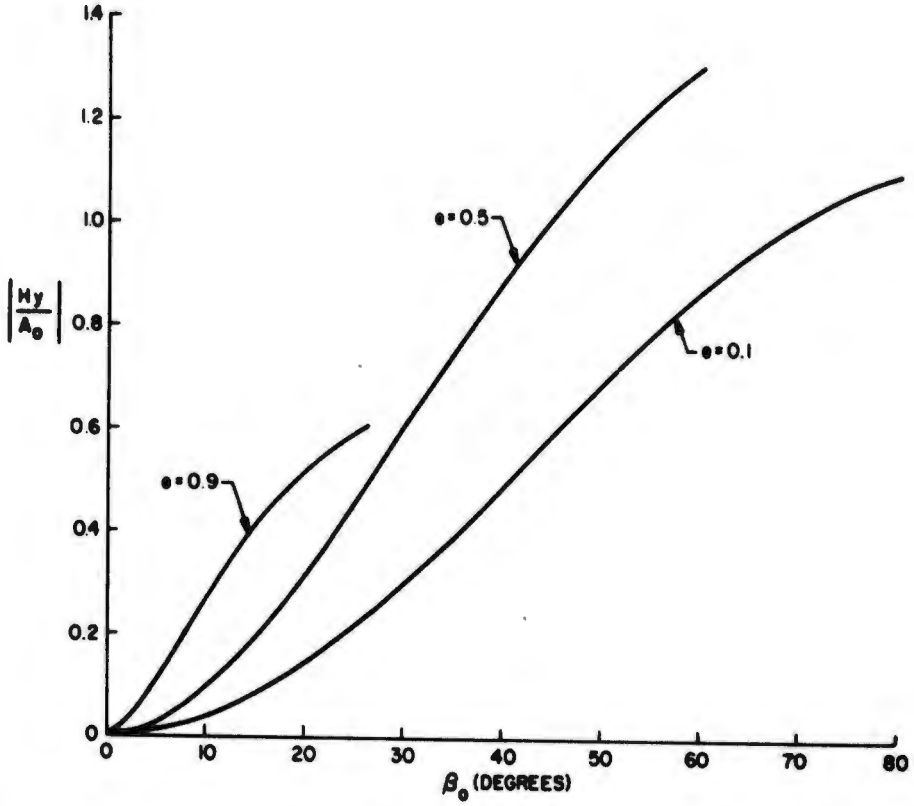

Figure 16. Magnitude of the Magnetic Field Produced at F_2 When an Ellipsoid of Revolution is Fed by an Isotropic Source at F_1

3.3 Field Near the Focus F_2

Unfortunately, Eq. (43) cannot be readily evaluated, either numerically or in closed form, for arbitrary values of p, ℓ, and β_o. However, when $p/r_2 \ll 1$, $kp^2/r_2 \ll 1$, $\ell/r_1 \ll 1$ and $k\ell^2/r_1 \ll 1$, it is acceptable to expand $k(\rho + u)$ in a Taylor series as $k(\rho + u) = \psi_1(\beta) - Q(\beta) \cos(\phi + \Delta)$, where $\psi_1(\beta) = k[2a - p \cos\eta \cos\beta - (\ell s/\tau) \cos\gamma]$ and

$$Q(\beta) = k \sin\beta \left[p^2 \sin^2\eta + \frac{\ell^2 b^4}{\tau^2} \sin^2\gamma + \frac{2 p \ell b^2 \sin\eta \sin\gamma}{\tau} \cos(\phi_1 - \phi_2) \right]^{1/2} \tag{50}$$

$$\tan\Delta = \frac{p\tau \sin\eta \sin\phi_2 + \ell b^2 \sin\gamma \sin\phi_1}{p\tau \sin\eta \cos\phi_2 + \ell b^2 \sin\gamma \cos\phi_1} \quad . \tag{51}$$

We now use this result in Eq. (43) and approximate ρ by r_2 and u by r_1 in the denominator of Eq. (43). We also assume that $G(\beta, \phi) = G(\beta)$ and that $D \simeq 1$. We can then perform the ϕ integrations in Eq. (43) to obtain

$$H_x(P_2) = \frac{ikb^4}{2} \int_0^{\beta_o} \frac{d\beta\, G(\beta)\, \bar{\gamma}_2}{r_1 r_2^2} \{\sin 2\Delta \sin\beta\, J_2(Q)(z' + c)$$

$$- 2iy' \cos\beta \cos\Delta\, J_1(Q)\} \exp[-i\psi_1(\beta)] \quad , \tag{52}$$

$$H_y(P_2) = \frac{ikb^4}{2} \int_0^{\beta_o} \frac{d\beta\, e^{-i\psi_1}\, G(\beta)}{r_1 r_2^2} \{\bar{\gamma}_2(z' - z) \sin\beta[J_o(Q) + \cos 2\Delta\, J_2(Q)]$$

$$+ 2v_2(z' - z)\, J_o(Q) + 2i x' \bar{\gamma}_2 \cos\beta \cos\Delta\, J_1(Q)$$

$$- \alpha b^2 \bar{\gamma}_2 \sin\beta \cos\beta[J_o(Q) - \cos 2\Delta\, J_2(Q)]\} \quad , \tag{53}$$

$$H_z(P_2) = -\frac{ikb^4}{2} \int_0^{\beta_o} \frac{d\beta\, e^{-i\psi_1}\, G(\beta)}{r_1 r_2^2} \{y' \bar{\gamma}_2 \sin\beta[J_o(Q) + \cos 2\Delta\, J_2(Q)]$$

$$+ 2v_2 y' J_o(Q) + i2\alpha b^2 \sin\beta \sin\Delta (v_2 + \bar{\gamma}_2 \sin\beta) J_1(Q)$$

$$+ x' \bar{\gamma}_2 \sin\beta \sin 2\Delta\, J_2(Q)\} \quad , \tag{54}$$

where $r_1 = 2a - r_2$, $r_2 = \alpha b^2$, $\gamma_2 = \bar{\gamma}_2 \cos\phi$, J_0, J_1, J_2 are Bessel functions, and $v_2 = \alpha^3 \cos\beta \sin\beta (\cos\beta - e)$.

When the angle, β_o subtended at F_2 by the reflector is small compared with unity, we can evaluate Eqs. (52) to (54) for the field in the focal plane, and also for the axial field near the focus F_2. In particular, let us assume that $\beta_o \ll 1$, $p/\lambda \ll \beta_o^{-3}$, $\ell/\lambda \ll \beta_o^{-3}(a + c)(a - c)^{-1}$ and $e\beta_o^2(1 - e)^{-2} < 1$. If we also assume that the feed lies in the plane transverse to the z-axis at F_1 and that the field point lies in the plane transverse to the z-axis at F_2 (so that $\gamma = \eta = \pi/2$) we find, provided $G(\beta)$ is isotropic,

$$H_x(P_2) \simeq - i \frac{a}{b^2} \Lambda \beta_o \cos \Delta \frac{J_2(\mu)}{\mu} p \sin \phi_2 \tag{55}$$

$$H_y(P_2) \simeq - \Lambda \left[\frac{J_1(\mu)}{\mu} - i \frac{a}{b^2} \beta_o \cos \Delta \frac{J_2(\mu)}{\mu} p \cos \phi_2 \right] \tag{56}$$

$$H_z(P_2) \simeq - \Lambda \left[\frac{p}{s + c} \frac{J_1(\mu)}{\mu} + i \beta_o \sin \Delta \frac{J_2(\mu)}{\mu} \right] \tag{57}$$

where

$$\mu = \beta_o Q_o \quad , \quad \Lambda = 2\beta_o^2 A_o (1 + e)(1 - e)^{-1}$$

and

$$Q_o = k \left[p^2 + \ell^2 \left(\frac{1 + e}{1 - e} \right)^2 + 2 p \ell \left(\frac{1 + e}{1 - e} \right) \cos (\phi_1 - \phi_2) \right]^{1/2} \tag{58}$$

and A_o as defined in Eq. (49). In deriving Eqs. (55) to (57), we have neglected higher order terms in β_o. Some plots of the results in Eq. (55) to (57) are shown in Figures 17 and 18, for the case when $\phi_2 = \pi/4$ and the source is located at F_1. Upon comparing these two figures, we see that the ratio of H_x and H_z to H_y depends quite strongly on the value of ka.

It is clear from Figures 16 and 17 that near F_2 the largest field component is H_y, and this is dominated by the term $J_1(\mu)/\mu$. Therefore the center of the focal spot occurs, approximately, at the point where $\mu = 0$. From Eq. (58) we see that this means that if the feed is located at (ℓ, ϕ_1) the center of the focal spot is at

$$p = \left(\frac{1 + e}{1 - e} \right) \ell \quad , \tag{59a}$$

$$\phi_2 = \phi_1 + \pi \quad . \tag{59b}$$

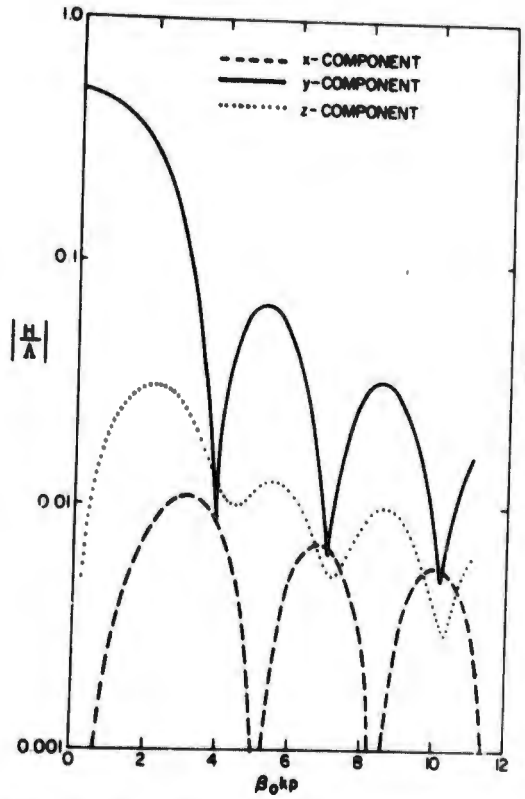

Figure 17. Magnetic Field Distribution in the Transverse Plane Passing through F_2 (that is, $\eta = \pi/2$) for the Case when $\phi_2 = 45^o$, $ka = 62.8$, $\beta_o = 10^o$, and $e = 0.8$

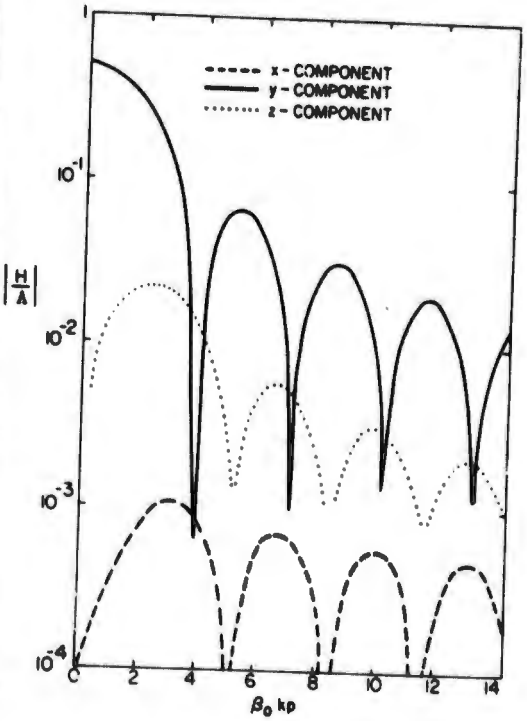

Figure 18. Magnetic Field Distribution in the Transverse Plane Passing through $F_2(\eta = \pi/2)$ for the Case when $\phi_2 = 45^o$, $ka = 628$, $\beta_o = 10^o$, and $e = 0.8$

Similarly the radius of the focal spot is determined from the first zero of $\mu^{-1} J_1(\mu)$. This is

$$\delta p \simeq \frac{3.83}{\beta_o k} \tag{60}$$

This result is consistent with Figures 17 and 18.

Because the magnetic field of the feed has only y and z components, the x-component of the magnetic field scattered by the reflector gives us one possible measure of the cross-polarization. Consequently, we shall define the cross-polarization ϵ_p as the ratio of the maximum value of H_x to the value of H_y at the center of the focal spot. We find

$$\epsilon_p = \frac{1}{2ka(1 - e^2)} \tag{61}$$

As expected, the cross-polarization vanishes when $ka \to \infty$, and increases as $e \to 1$.*

We can also evaluate the β-integration in Eqs. (50) to (52) for the case when the source point and the field point lie on the z-axis. The result is

$$H_x = H_z = 0 \tag{62a}$$

$$H_y(P_2) \simeq -A_o \beta_o^2 \left(\frac{1 + e}{1 - e}\right)\left[1 - \frac{p \cos \eta}{a + c}\right] \operatorname{sinc}\left(\frac{m\beta_o^2}{2}\right) e^{ik(p \cos \eta + \ell \cos \gamma - m\beta_o^2/2k)} \tag{62b}$$

where

$$k[p \cdot \cos \eta + \ell(1 + e)^2(1 - e)^{-2} \cos \gamma]/2 \quad .$$

From Eq. (62b) we see that if the source is displaced from F_1 by a distance ℓ towards ($\gamma = 0$), the reflector the center of focal spot is displaced from F_2 by a distance $(1 + e)^2(1 - e)^{-2}\ell$ away from the reflector ($\eta = \pi$). Also, we define the depth of focus at F_2 as the distance from the center of the focus to the first zero of sinc $(\beta_o^2 m/2)$. We get†

$$\delta p = \pm \frac{2\lambda}{\beta_o^2} \quad . \tag{63}$$

This result is consistent with the exact results in Figures 14 and 15.

---

*Note, however, that our results are not valid when e is too near unity, because we have assumed $e\beta_o^2(1 - e)^{-2} < 1$.

†When β_o is not small, we get

$$\delta p \simeq \pm \frac{\pi}{k \sin^2\left(\frac{\beta_o}{2}\right)}$$

3.4 Evaluation by Stationary Phase

When $k(\rho + u - 2a) \gg 1$, or equivalently* $kp \gg 1$, we may evaluate Eqs. (52) to (54) for the field near the focus by the method of stationary phase, even for the case when β_o is not small. If we assume that η and γ are not equal to 0 or π, so that $Q \gg 1$, we may use the asymptotic expansions for the Bessel functions in Eqs. (52) to (54). In that case, we find that the integrals over β have a stationary point when $d/d\beta(\psi + Q) = 0$. For the case when $\ell = 0$ (source point at F_1) and $\beta_o \leq \pi/2$, we then find that there is a stationary point at $\beta = \eta$ if $0 < \eta < \pi/2$ and at $\beta = \pi - \eta$ if $\pi/2 < \eta < \pi$. This means that if $\beta_o \leq \eta \leq \pi - \beta_o$ there is no stationary point within the range of integration in Eqs. (52) to (54) and the only contribution to the integral comes from the end point at $\beta = \beta_o$ (that is, from the rim of the reflector). There is no contribution from $\beta = 0$ because the integrand vanishes there. The aforementioned conclusions are essentially the same as those obtained in Section 2.4, and consequently Figure 10 is appropriate for both the elliptic cylinder and the ellipsoid of revolution, provided we set $\beta_1 = \beta_o$ in Figure 10.

As an example of the results one obtains by using the method of stationary phase, let us compute the cross-polarized component H_x. If $\ell = 0$ (feed at F_1) and we assume that† $0 < \eta < \beta_o$ we find from Eq. (52)

$$H_x(P_2) = H_x^g(P_2) + H_x^E(P_2) \tag{64}$$

where H^g is the contribution to the magnetic field from the ring on the reflector at $\beta = \eta$. This is given by

$$H_x^g(P_2) = \frac{-2\, b^4\, G(\eta)\, \bar{\gamma}_2(\eta)\, e^{-i2ka} \cos\eta \cos\phi_2 \sin\phi_2}{r_1(\eta)\, r_2^2(\eta)} \tag{65}$$

where $\bar{\gamma}_2(\eta)$ means that, in the expression for $\bar{\gamma}_2$, β is replaced by η. The quantity H^E is the contribution to the field from the rim of the reflector, and is given by

---

*Note that it is possible to have $kp \gg 1$ even though $p \ll (a + c)$ and $kp^2 \ll (a + c)$ required for Eqs. (52) to (54) to be valid.

†The method of stationary phase is not valid for η near zero because Q is no longer large there. Also the result in Eq. (64) is not valid for η near β_o. A special treatment is required for this case (that is, stationary point approaching end point).

$$H_x^E(P_2) = \frac{b^4\, G(\beta_o)\, \bar{\gamma}_2(\beta_o) \sin\phi_2 \cos\phi_2\, e^{-i2ka}}{(2\pi kp \sin\eta \sin\beta_o)^{1/2}\, r_1(\beta_o)\, r_2^2(\beta_o)}$$

$$\cdot\, [\sin(\beta_o + \eta)\, Y(\beta_o - \eta) + \sin(\beta_o - \eta)\, Y(\beta_o + \eta)] \tag{66}$$

where

$$Y(\beta) = \frac{e^{i(kp\cos\beta - \pi/4)}}{\sin\beta} \tag{67}$$

For $\beta_o < \eta < \pi - \beta_o$ there is no stationary point within the range of integration, and then

$$H_x(P_2) = H_x^E(P_2) \tag{68}$$

In the limit when $\beta_o \ll 1$ and $\eta = \pi/2$, we can readily show that Eq. (68) reduces to the asymptotic expansion of Eq. (55). Therefore, the results obtained by the method of stationary phase are consistent with those obtained in Section 3.3. Unfortunately, because Eqs. (52) to (54) require that $1 \ll (a + c)$ and so on, our stationary phase results also require that $p \ll (a + c)$, but we have no restriction on the magnitude of β_o.

3.5 Evaluation of Eq. (43) for $p \to \infty$

If $\ell = 0$ (source at F_1) and the field point is in the Fraunhofer zone of the reflector, we can expand ρ in the Taylor series as $\rho = p - r_2 \cos\eta \cos\beta - r_2 \sin\beta \sin\eta \cos(\phi - \phi_2)$. If we use this result in Eq. (43) and then perform the integrations over $d\phi$ we obtain after considerable manipulation

$$\underline{H}(p \to \infty) = \frac{ikb^4}{2p} \int_0^{\beta_o} \frac{G(\beta)\, d\beta\, e^{-ik(p + a\tau - r_2\cos\eta\cos\beta)}}{a\tau}$$

$$\cdot\, \{\hat{x}\, \bar{\gamma}_2 \sin 2\phi_2 [\sin\beta \cos\eta\, J_2(V_o) + i \sin\eta \cos\beta\, J_1(V_o)]$$

$$+ \hat{y}\left[(\bar{\gamma}_2 \sin\beta\cos\eta + 2v_2\cos\eta)\, J_o(V_o) + \bar{\gamma}_2 \sin\beta\cos\eta\cos 2\phi_2\, J_2(V_o)\right.$$

$$\left. + 2i\bar{\gamma}_2 \sin\eta\cos\beta\cos^2\phi_2\, J_1(V_o)\right]$$

$$- \hat{z}\left[(\bar{\gamma}_2 \sin\beta + 2v_2)\sin\eta\sin\phi_2\, J_o(V_o) - \bar{\gamma}_2 \sin\eta\sin\beta\sin\phi_2\right.$$

$$\left. J_2(V_o)\right]\Bigg\} \qquad (69)$$

where $V_o = kr_2 \sin\beta \sin\eta$. If $kr_2 \gg 1$ and η is not too near to 0 or π, we can evaluate Eq. (69) by the method of stationary phase. If we use the asymptotic expansions for the Bessel functions in Eq. (69), we find that the stationary point β_s is given by $\beta_s = \sin^{-1}(\sin\eta/D_o) - \sin^{-1}(e\sin\eta/D_o)$ where $D_o = (1 + e^2 + 2e\cos\eta)^{1/2}$. For $\pi/2 < \eta < \pi$ this result can be approximated by $\beta_s = \pi - \eta$. Therefore if* $\eta > \pi - \beta_o$ there is a stationary point within the range of integration in Eq. (69) and the field at P_2 is due to both the stationary point contribution plus the contribution from the rim of the reflector. For $\eta < -\pi - \beta_o$ the stationary point does not lie within the range of integration, and the only contribution to the far field comes from the rim of the reflector. These conclusions are illustrated graphically in Figure 19.

Because there are different lengthy expressions for the field for each range of η, we have chosen not to write them here, but they follow readily by applying the standard stationary phase[8] formulae to Eq. (69).

When $\eta = \pi$ so that the field point for $p \to \infty$ lies on the z-axis we can evaluate Eq. (43) directly. We find that $H_x = H_z = 0$. Also for $\beta_o \ll 1$ and $G(\beta) = G(0)$ we can approximate H_y as (provided $a\cos\beta_o > c$)

$$H_y(p \to \infty) = \frac{2iG(0)}{p}\left(\frac{1+e}{1-e}\right) e^{-ik(p+2a-g/k)}$$

$$\cdot \left[\left(1 - \frac{a_c\beta_o^2}{2}\right)\sin g + i\frac{a_o\beta_o^2}{2}\cos g\right] \qquad (70)$$

where $g = ka(1+e)\beta_o^2/4$ and $a_o = 0.5(1 + 2e - e^2)(1-e)^{-2}$. Equation (70) is valid provided $e\beta_o^2(1-e)^2 < 1$ and $ka\beta_o^4/24 \ll 1$.

---

*Note that for η near π we cannot use the stationary phase method, because the asymptotic expansion of the Bessel functions is invalid there.

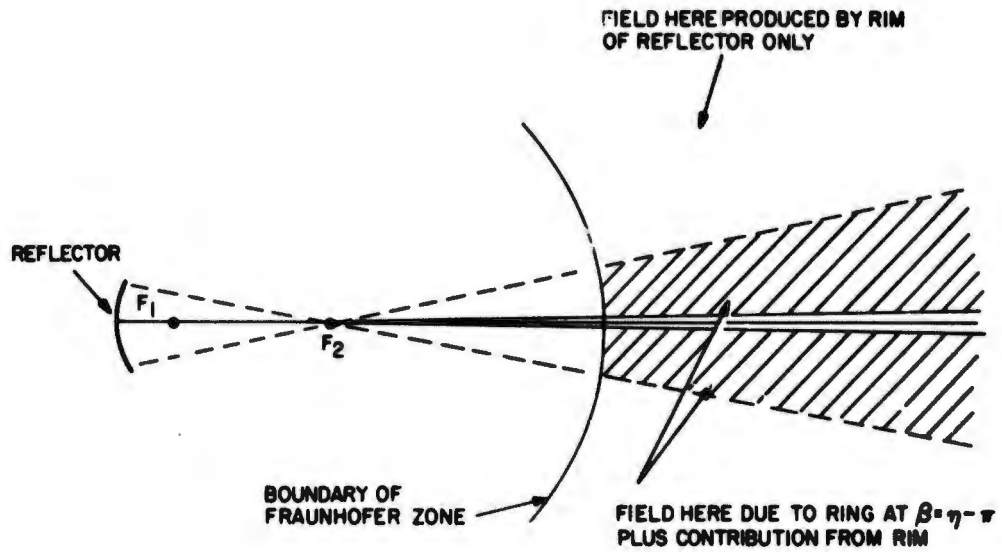

Figure 19. Pictorial Illustration of the Portions of the Ellipsoid which Contribute to the Far Field

Before concluding this section on the far fields distribution, we comment that the stationary phase evaluation of Eq. (69) is also applicable in the shadow of the reflector. In this region there is no stationary point contribution, and the only contribution comes from the rim of the ellipsoid. The physical optics diffraction coefficient for the rim is again (as in Section 2.4) nearly equal to the diffraction coefficient calculated via the geometrical theory of diffraction, provided $\beta_o < (1 - e)(1 + e)^{-1}$.

4. DISCUSSION AND CONCLUSIONS

Among the conclusions we have reached is that, except very near to the focal regions, the fields of a large elliptical reflector can be adequately evaluated by the method of stationary phase. Although we have demonstrated this here only for the ellipse, it is interesting to note that we have also performed these calculations for a paraboloid which is illuminated by a plane wave; we found that the results calculated by the stationary phase approach agreed quite well with exact computer[12] calculations of the near field distribution.

---

12. Fante, R. (1977) Near field distribution of a paraboloidal reflector, IEEE Trans. Ant. Prop. 25:589-590.

In this paper, we have tried to limit our study to a diffraction analysis of the elliptical reflector. In general, we have not resorted to any optical methods. For example, the motion of the focal spot as a function of feed position could also have been accomplished using standard optical techniques, as outlined by Sletten.[2]

Finally, we comment that although many authors present electric field distributions, we have found it more convenient to present the magnetic field distributions. The electric field can readily be calculated from $\underline{H}$ via the Maxwell curl equation $\underline{E} = (i\omega\epsilon_o)^{-1} \nabla \times \underline{H}$. For the sake of conciseness, we have omitted the expressions for the electric field.

References

1. Soejima, T. (1973) Scattering by two elliptical reflectors; correspondence with diffraction by two circular apertures, IEEE Trans Ant. Prop. 21:110-113.
2. Sletten, C.J. (1969) Reflector antennas, in Antenna Theory, Part 2, R. Collin and F. Zucker, Ed., McGraw-Hill, New York.
3. Minnett, H., and Thomas, B. Mac A. (1968) Fields in the image plane of symmetrical focusing reflectors, Proc. IEE 115:1419-1430.
4. Rusch, W., and Potter, P. (1970) Analysis of Reflector Antennas, New Academic Press, New York.
5. Clarricoats, P., and Poulton, G. (1977) High-efficiency microwave reflector antennas – a review, Proc. IEEE 65:1470-1504.
6. Silver, S. (1965) Microwave Antenna Theory and Design, Dover, New York.
7. Abramowitz, M., and Stegun, I., Ed. (1964) Handbook of Mathematical Functions, U.S. Govt Printing Office, Washington, D.C.
8. Felsen, L., and Marcuvitz, N. (1973) Radiation and Scattering of Waves, Prentice Hall, New York.
9. James, G., and Kerdemelidas, V. (1973) Reflector antenna radiation pattern analyzed by equivalent edge currents, IEEE Trans. Ant. Prop. 21:19-24.
10. Knop, C. (1976) On the front to back ratio of a parabolic dish antenna, IEEE Trans. Ant. Prop. 24:109-111.
11. Rusch, W. (1974) Antenna Notes, Vol II, NB. 846, Tech Univ., Lyngby, Denmark, 135-141.
12. Fante, R. (1977) Near field distribution of a paraboloidal reflector, IEEE Trans. Ant. Prop. 25:589-590.